Copyright WILEY-VCH Verlag GmbH & Co. KGaA, 69469 Weinheim, Germany, 2012.

NANO MICRO small

Supporting Information

for *Small*, DOI: 10.1002/smll.201101739

Tunable Aqueous Virtual Micropore

*Jae Hyun Park, Weihua Guan, Mark A. Reed, and Predrag S. Krstic´**

Supplementary Information for "Tunable Aqueous Virtual Pore"

Jae Hyun Park[1], Weihua Guan[2], Mark A. Reed[2,3] and Predrag S. Krstić[1]*

[1] Physics Division, Oak Ridge National Laboratory, Oak Ridge, TN 37831

[2] Department of Electrical Engineering, Yale University, New Haven, CT 06520

[3]Department of Applied Physics, Yale University, New Haven, CT 06520

*Corresponding Author: krsticp@ornl.gov

SI1. Stability of Aqueous Quadrupole Trap

SI2. Details for the Equation of Motion, Equation (1) and Random Force

SI3. Clausius-Mossoti Factor

SI4. RMS fluctuation v.s. q for EP-only cases

SI5. Estimations of rms Fluctuations with Variable Charges

SI6. Mean and Width of Radial Distribution of Particles

SI7. Trap Stiffness and Effects of Particle Size in AVP

SI1. Stability of Aqueous Quadrupole Trap

The stability of AQT is different from the conventional Paul trap in vacuum or low-pressure gaseous medium, due to the presence of dielectrophoretic (DEP) force in addition to the electrophoretic (EP) force. Also, as mentioned in the text, the stability of AQ trap is determined by the mean motion (without random motion) of the particle under the assumption that the trap size is much larger than the random fluctuations. The equation of motion (EOM) in AQ trap including DEP as well as AC EP forces has the following form:

$$\frac{d^2x}{d\tau^2} = -b\frac{dx}{d\tau} + 2q\cos(2\tau)x + r_m\left[\mathrm{Re}(f_{CM}) + \mathrm{Re}(f_{CM})\cos(4\tau) - \mathrm{Im}(f_{CM})\sin(4\tau)\right]x \quad , \tag{SI1.1}$$

with introducing the dimensionless parameters of

$$\tau = \frac{\Omega}{2}t, b = \frac{2\xi}{M\Omega}, q = \frac{2QU}{MR_0^2\Omega^2}, r_m = \frac{4\alpha_m}{M\Omega^2}. \tag{SI1.2}$$

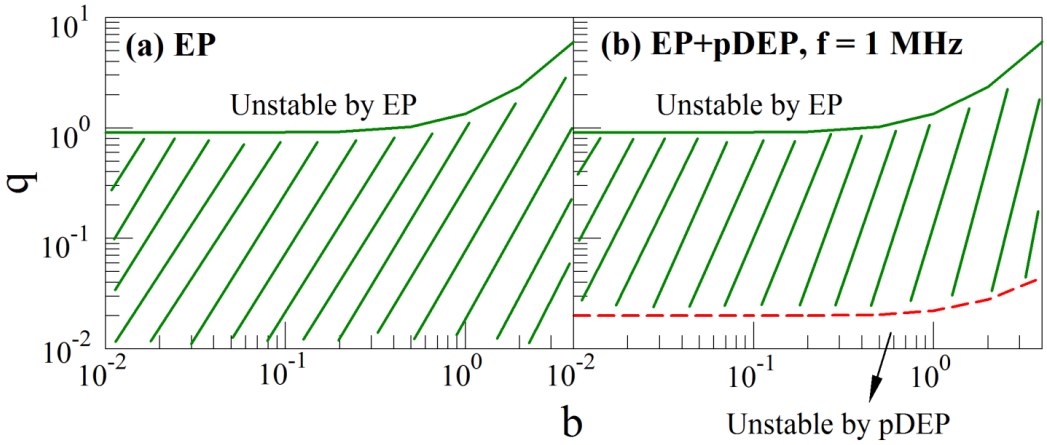


Figure S1. b-q Stability diagrams with a = 0.0 with/without pDEP: (a) EP; (b) EP+pDEP with f = 1.0 MHz. The lines are the stability borders. The green line is the stability border due to quadrupole electric field and the red dashed line is the border due to pDEP. The stable regions are the regions between the two borders (slanted lines).

By solving the EOM in Equation (SI1.1) and investigating the particle trajectory in long-time limit, we can determine the stability of trap. If the particle approaches the origin in long-time limit, the system is in the stable region for a given combination of b and q parameters. If the particle trajectory diverges from the origin, the system is unstable. The stability border is the (b,q)-relationship in which the trajectory keep oscillating without converging or diverging. The resultant (b,q)-stability diagram is shown in Figure S1. As shown in the Figure S1, for

small q's a new unstable region is generated whereas for the large q's the stability border is not influenced by the presence of DEP.

SI2. Details for the Equation of Motion, Equation (1)

The original two-dimensional equation of motion for the particle in AQT is given as:

$$\frac{d\,\mathbf{r}}{d\,\tau^2} = -b\frac{d\,\mathbf{r}}{d\,\tau} + 2q\cos 2\tau\left(x\hat{\mathbf{e}}_x - y\hat{\mathbf{e}}_y\right) + r_m\left[\mathrm{Re}\left(f_{CM}\right)\left(1+\cos 4\tau\right) - \mathrm{Im}\left(f_{CM}\right)\sin 4\tau\right]\left(x\hat{\mathbf{e}}_x - y\hat{\mathbf{e}}_y\right) \tag{SI2.1}$$

where $\mathbf{r} = x\hat{\mathbf{e}}_x + y\hat{\mathbf{e}}_y$ is the transformed coordinate vector. Here, x is the transformed coordinate in x-direction defined as x=(MΩ/2)X where X presents the physical coordinate and y is the transformed coordinate in y-direction defined as y=(MΩ/2)Y where Y presents the physical coordinate. τ = (Ω/2)t is the dimensionless time, ξ is the friction coefficient of a non-slip spherical particle in Stokes' drag, ξ=6πηa, where viscosity of medium, a is the particle radius. In the main text, we presents the x-component of Eq. (SI2.1). We also checked the results from y-component equation, however they did not change.

R is the white random force [S1] which vanishes in the mean:

$$\left\langle R(t)\right\rangle = 0, \tag{SI2.2}$$

and which is uncorrelated with the velocity $v(t)$ at any earlier time:

$$\left\langle v(t)R(t')\right\rangle = 0 \qquad t' > t. \tag{SI2.3}$$

where <> means the statistical average over an ensemble of particles. Finally, correlation time of R is infinitely short, namely the autocorrelation function of R(t) has the form,

$$\left\langle R(t)R(t')\right\rangle = G_R\delta(t-t'). \tag{SI2.4}$$

G_R is the constant spectral density in power spectrum of the random force. Kubo [S2] showed using fluctuation-dissipation theorem that G_R is related to the friction coefficient by

$$G_R = 2k_BT\xi. \tag{SI2.5}$$

The DEP force is not a function of charge. Since EOM in y-direction differs only in the sign of q-parameter and the stability diagram is symmetric with respect to q = 0, [S3] it is sufficient to solve the EOM in one direction (e.g. x).

SI3. Clausius-Mossoti Factor

Clausius-Mossoti factor is defined as $f_{CM} = \frac{\tilde{\varepsilon}_p - \tilde{\varepsilon}_m}{\tilde{\varepsilon}_p + 2\tilde{\varepsilon}_m}$ with $\tilde{\varepsilon} = \varepsilon_0 \varepsilon - j\frac{\sigma}{\Omega}$ where ε is relative dielectric constant and ε_0 is the vacuum permittivity (ε_0 = 8.85×10^{-12} F/m). The subscript p and m presents particle and medium, respectively. σ is the electric conductivity of material. j is imaginary unit $\left(j = \sqrt{-1}\right)$.

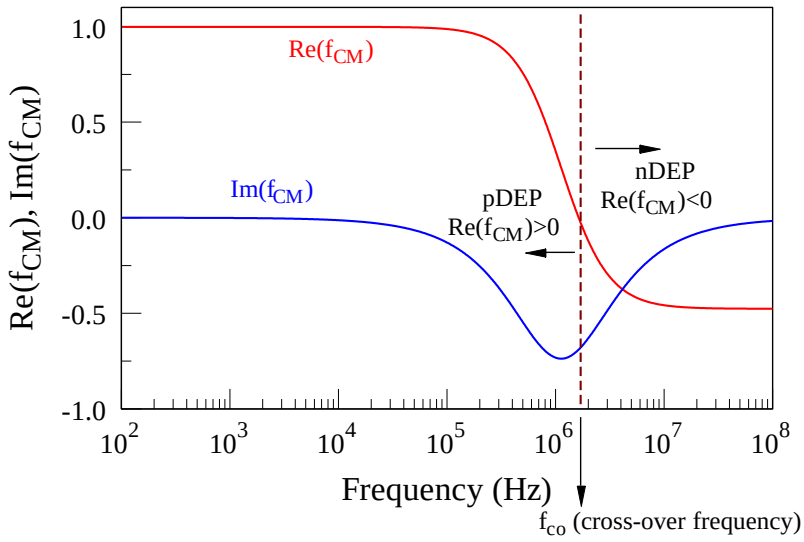


Figure S2. Typical Variation of Clausius-Mossoti (CM) factor, f_{CM}, with driving frequency. Re(f_{CM}) is the real and Im(f_{CM}) is the imaginary part of the f_{CM}, respectively. The cross-over frequency, f_{co}, indicates the frequency for which the sign of Re(f_{CM}) changes. For $f < f_{co}$, Re(f_{CM}) > 0 and the dielectrophoretic force acts toward the electrode (high electric field region), producing positive dielectrophoresis (pDEP) while for $f > f_{co}$, Re(f_{CM}) < 0 and the dielectrophoretic force acts toward the trap centre (low electric field region), producing negative dielectrophoresis (nDEP). For the polystyrene bead in aqueous medium, ε_p = 2.55 ε_m = 78.5 σ_p = 0.01 S/m σ_m = 5.5×10^{-6} S/m,[S4,S5] and the cross-over frequency is 1.63 MHz.

SI4. RMS Fluctuation v.s. q for EP-only Cases

The rms fluctuations without DEP can be calculated by solving Equation (1) with r_m = 0,

$$\frac{d^2x}{d\tau^2} + b\frac{dx}{d\tau} - 2q\cos(2\tau)x = \frac{2}{\Omega}R\left(\frac{2\tau}{\Omega}\right) \qquad \text{(SI4.1)}$$

The definitions of non-dimensional variables in the equation are explained in the main text and in SI3. Arnold *et al.* [S6] proposed an efficient numerical algorithm using Green function transformation and random phase approach, and we recently derived a closed form of rms fluctuations with Mathieu sine and cosine functions. We implemented both methods to

compute the rms fluctuations for various b and q parameters. Figure S3 shows the variation of rms fluctuations with q-parameters for three b-values of b = 1.0, 2.0, and 4.0. For all b-parameters, the rms fluctuations decrease with increase of q, reach the minima, and diverge.

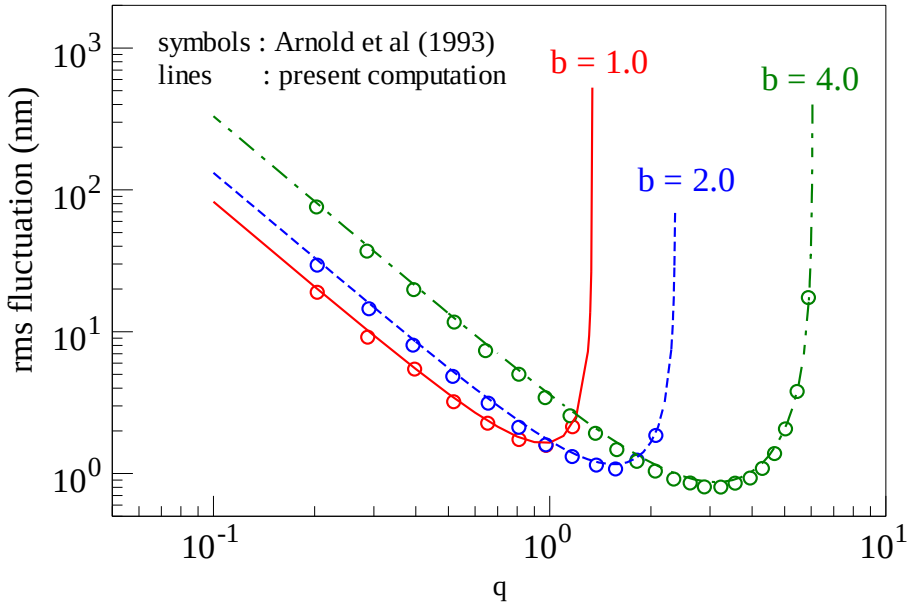


Figure S3. Variation of the rms fluctuations with q for three b-values of b=1.0, 2.0, and 4.0, The rms fluctuations are computed for the polystyrene bead whose radius is 490 nm and density of 1050 kg/m^3. The viscosity of medium is 0.89×10^{-3} Pa·s.

SI5. Means and Widths of the Radial Distributions of Particle

This section shows the means and widths of radial distributions of a particle in an aqueous virtual pore, due to the rms fluctuations. The mean value is defined as $\bar{r} = \left(\sum_{i=1}^{N} r_i\right) \Big/ N$ where N is the total number of events and r_i is the radial position of particle in each event. The width of radial distribution in Figure 2b and Figures 3(b-e), w_r, is defined as the standard deviation of the distribution, $w_r = \sqrt{\sigma_{rr}^2} = \sqrt{\left[\sum_{i=1}^{N}\left(r_i^2 - (\bar{r})^2\right)\right] \Big/ N}$.

Figures S4(a-b) show the profiles of mean (a) and the width (b) for Figure 2(b-c) in which the voltage varies with a fixed frequency. Figures 4(c-d) show the profiles of means (c) and the widths (d) for Figure 3(b-e) in which the frequency varies with a fixed voltage. The distributions of the calculated and measured means are similar, if the particle charge is properly chosen. For the fixed frequency cases (Figures S4a and b), the proper charge is

8×10^4 *e* while for the fixed voltage cases (Figures S4c and d), the proper charge is 4×10^4 *e*. The widths of the distributions are about a half of the means.

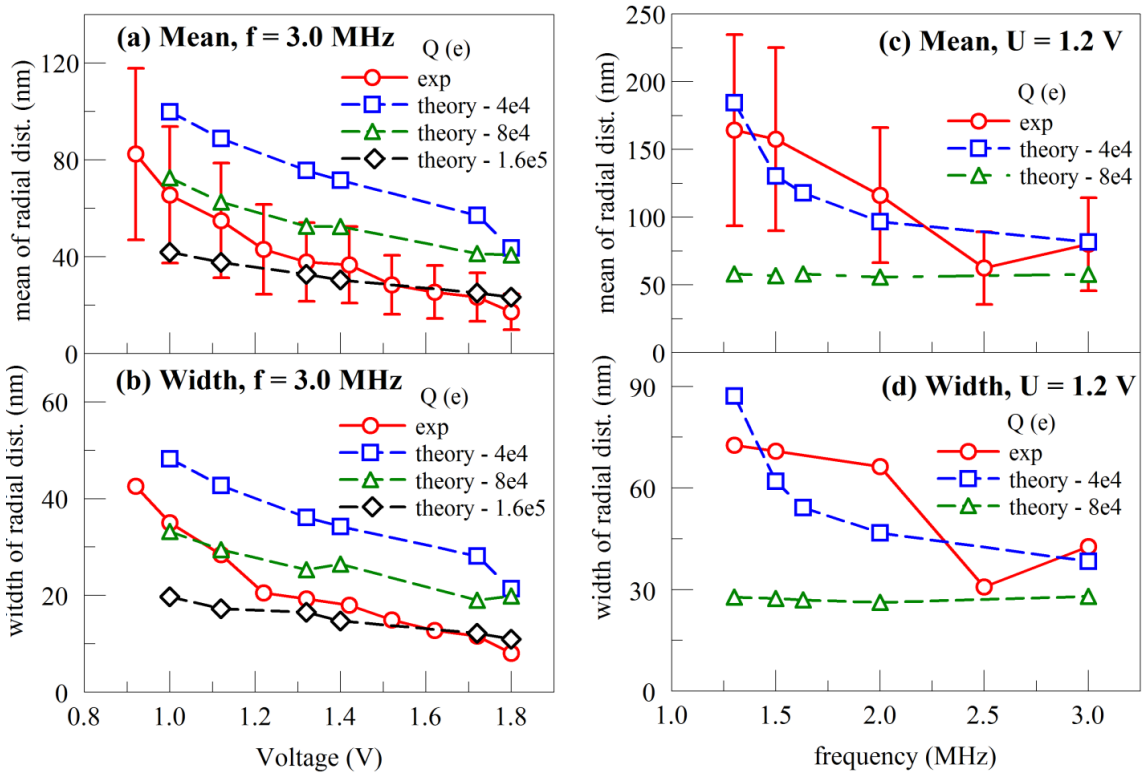


Figure S4. Measured and calculated means and widths of radial distributions when varying AC voltage and frequency: (a) means and (b) widths of radial distributions for a fixed frequency of f = 3.0 MHz. (c) mean and (d) width of radial distributions for a fixed voltage of U = 1.2 V. The error margins of the experimental data in (a) and (c) are about 40%.

SI6. Estimations of RMS Fluctuations with Variable Charges

In Figure 2a, we assumed that the charge is fixed regardless the variation of applied voltage. However, the comparison strongly suggests the possibility of variable charges depending on AC voltage. We selected four voltages of 1.0, 1.12, 1.32, and 1.72 V, for which the measured values exist. The estimation of the rms fluctuations with variable charges consists of three steps described in Figure S5. The first step is to construct the fitting relations between Q and rms fluctuations, modelled as $\sqrt{\bar{\sigma}_{xx}^{\infty}} = aQ^b$, for four different U's (Figure S5a). Interestingly, the exponents are always same as -0.62, while the pre-factor, *a*, is varied depending on the voltage. The second step is to build the fitting relation between U and Q, which can be successfully modelled with a linear relation $\frac{Q}{10^5 e} = cU + d$ (Figure S5b).

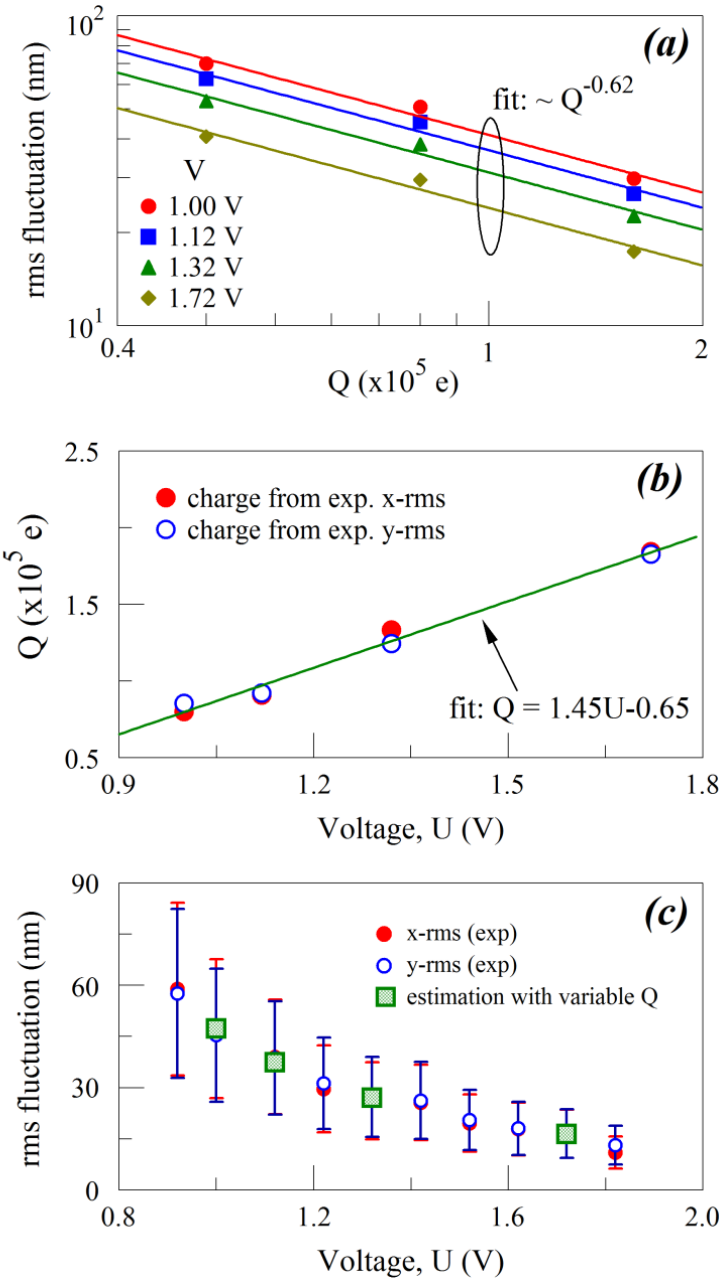


Figure S5. Estimation of rms fluctuations with variable charges: (a) STEP 1 – construction of fitting relations between Q and rms fluctuation for four different AC voltages of 1.0, 1.12, 1.32, and 1.72 V. The selected relation is $\sqrt{\bar{\sigma}_{xx}^{\infty}} = aQ^b$ for each voltage. The exponents of fitting relations are always obtained as -0.62 regardless of the voltage while the *a*-values are ranging from 41.25, 36.83, 31.25 to 24.00 nm with variation of voltages from 1.0, 1.12, 1.32, to 1.72 V, respectively; (b) STEP 2 – build a fitting relation of $\frac{Q}{10^5 e} = cU + d$ between U and Q. The c and d-values are 1.44 [V^{-1}] and -0.65, respectively. The charge is computed using the relation in (a) and the measured rms fluctuations; (c) STEP 3 – estimation of the rms fluctuations using the variable charge given by the relation in (b).

The charges are computed from the relation of $\sqrt{\bar{\sigma}_{xx}^{\infty}} = aQ^b$. The fitting parameters are 1.44 V^{-1} and -0.65 for c and d, respectively. Finally, using the two latest relations ($\sqrt{\bar{\sigma}_{xx}^{\infty}} = aQ^b$ and $\frac{Q}{10^5 e} = cU + d$) we can re-construct the voltage versus voltage plot (Figure S5c), to check the quality of the fits.

SI7. Trap Stiffness and Effects of Particle Size in AVP

As discussed by Guan *et al.*, [S7] the trap stiffness is derived as $k_{EP} = \frac{Q^2 U^2}{2M\Omega^2 r_0^4 \left[1+\left(\xi/M\Omega\right)^2\right]}$ for EP and $k_{DEP} = \left|\mathrm{Re}\left(f_{CM}\right)\right| \frac{2\pi\varepsilon_m\varepsilon_0 a^3 U^2}{r_0^4}$ for DEP, from the consideration of pondermotive components of each force. When the surface charge and mass densities are maintained constant with varying trap size proportionally to the particle size, ($Q = 4\pi a^2\sigma_s$, $r_0 = 8a$, $M = \rho_p \frac{4}{3}\pi a^3$, and $\xi = 6\pi\eta a$), $k_{EP} \propto a$ while $k_{DEP} \propto 1/a$.

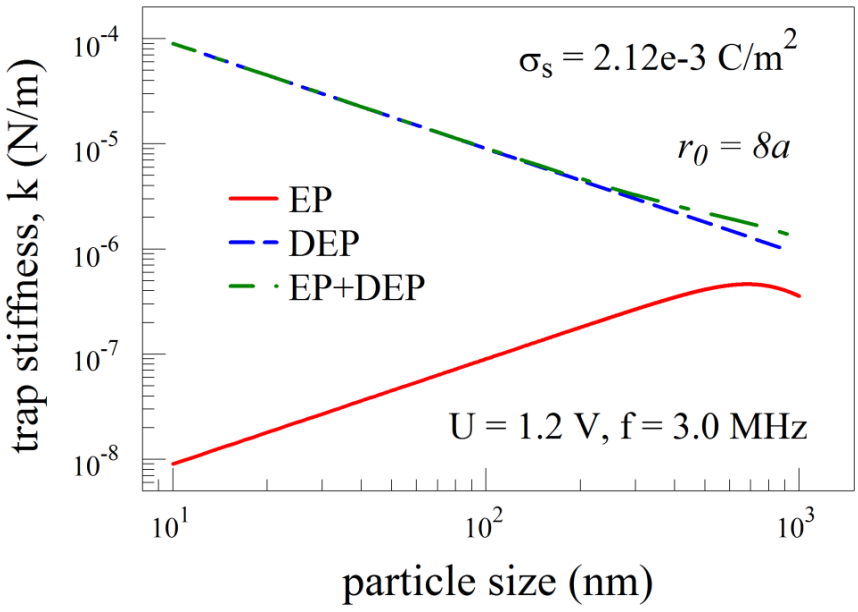


Figure S6. Variation of trap stiffness with the particle size. The particle is polystyrene with the density of 1050 kg/m^3. The trap size varies proportional to the particle size while the surface charge density is fixed as 2.12×10^{-3} C/m^2.

In Figure S7a, the surface charge density, σ_s, and the volume mass density, ρ_p, are maintained constant as in Figure S6. Note that in the experiment, the particle size is a = 490

nm and the trap size r_0 = 4 μm. This ratio is held fixed in all the calculations in Figure S7a. The EP rms fluctuations (r_m = 0) decrease with increase of the particle size whereas the DEP fluctuations (q = 0) increase with increase of the particle size. The total EP+DEP fluctuations ($q \neq 0$ and $r_m \neq 0$) increase with increase of particle size. However, the rms fluctuations increase with increase of the trap size, as shown in Figure S7b, while are reduced with increase of the particle charge (Figure S7c). In Figure 7d, we investigate the frequency effects for a small particle in a small trap ($2a$ = 10 nm and $2r_0$ = 81.63 nm) and a large particle in a large trap ($2a$ = 980 nm and $2r_0$ = 8 μm). For smaller case the AC voltage is reduced to 0.8 V to avoid the dielectric break-down in water.[S8] The rms fluctuations decrease with increase of frequency, and the decrement is significantly reduced for the smaller case.

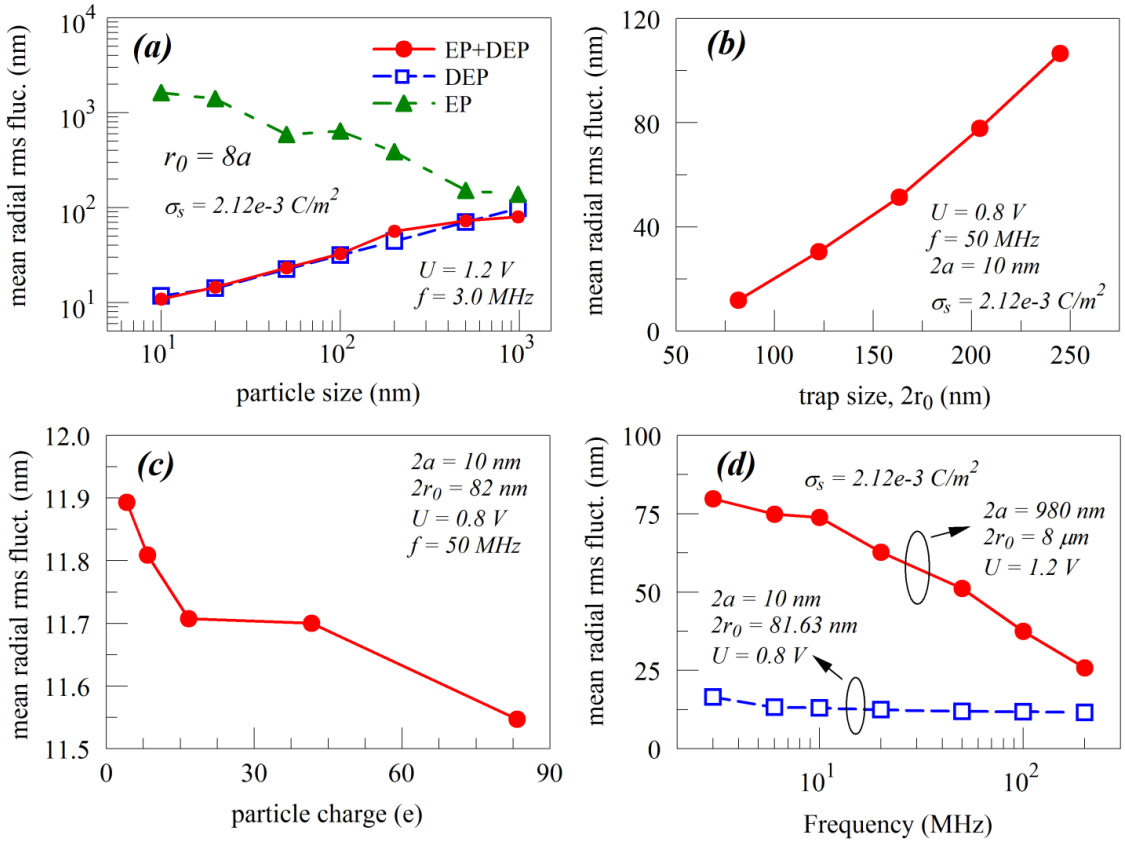


Figure S7: Variations of mean radial rms fluctuations with (a) particle size, (b) trap size, (c) particle charge, and (d) frequency.

References for Supplementary Information:

[S1] R. Kubo, *Rep. Prog. Phys*. **1996**, 29 255–284.

[S2] F. G. Major, V. N. Gheorghe, G. Werth, *Charged particle traps: physics and techniques of charged particle field confinement*, Springer, Berlin, **2005**.

[S3] W. T. Coffey, Yu. P. Kalmykov, J. T. Waldron, *The Langevin equation: with applications to stochastic problems in physics, chemistry and electrical engineering*, 2nd ed. World Scientific Publishing Co., Singapore, **2004**.

[S4] N. G. Green and H. Morgan, *J. Phys. Chem. B* **1999**, 103, 41-50.

[S5] S. Park and A. Beskok, *Anal. Chem.* **2008,** 80, 2832-2841.

[S6] S. Arnold, L. M. Folan, A. Korn, *J. Appl. Phys.*, **1993**, 74, 4291-4297.

[S7] W. Guan, J. H. Park, P. S. Krstić, M. A. Reed, *Nanotechnology*, **2011**, 22, 245103.

[S8] W. A. Stygar, T. C. Wagoner, H. C. Ives, Z. R. Wallace, V. Anaya, J. P. Corley, M. E. Cuneo, H. C. Harjes, J. A. Lott, G. R. Mowrer, E. A. Puetz, T. A. Thompson, S. E. Tripp, J. P. VanDevender, J. R. Woodworth, Phys. Rev. ST Accel. Beams **2006**, 9, 070401.